Langmuir

Article

pubs.acs.org/Langmuir

Surfactant-Induced Marangoni Eddies Alter the Coffee-Rings of Evaporating Colloidal Drops

Tim Still,* Peter J. Yunker, and Arjun G. Yodh

Department of Physics and Astronomy, University of Pennsylvania, Philadelphia, Pennsylvania 19104, United States, and Complex Assemblies of Soft Matter, CNRS-Rhodia-UPenn UMI 3254, Bristol, Pennsylvania 19007, United States

Supporting Information

ABSTRACT: The influence of the small ionic surfactant sodium dodecyl sulfate (SDS) on the evaporation of drying colloidal droplets is quantitatively investigated. The addition of SDS leads to a significantly more uniform deposition of colloidal particles after evaporation (i.e., the so-called "coffee-ring effect" is dramatically altered). We understand this phenomenon in the context of circulating radial Marangoni flows induced by the variation of SDS concentration along the air−water interface. Video microscopy permits the direct visualization of the colloidal particles involved in these flows, revealing a surprisingly stable "Marangoni eddy" that prevents particle deposition at the drop perimeter.

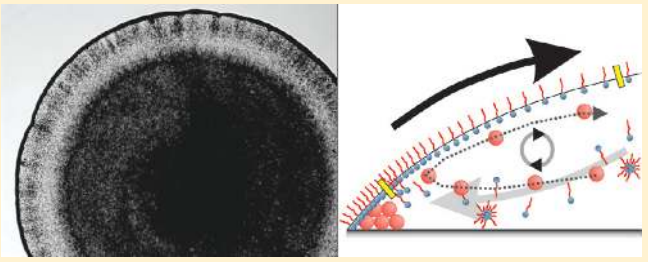

INTRODUCTION

A drying drop of coffee, tea, or water containing small solid particles typically leaves a thin ring-shaped stain, wherein most of the solid material is deposited after evaporation. This highly nonuniform deposition, known as the coffee-ring effect, is produced when the drop edges are pinned and subsequent radial capillary flows from the drop center to its edge carry suspended or dissolved solutes to the perimeter.[1−3] The effect is robust, persisting over many length scales of solid constituents (i.e., from micrometer-sized particles down to macromolecules) and across many different surfaces and interfaces (i.e., from concrete to glass to smooth mica[1,4−6]). The effect also influences practical applications that require uniform deposition, including printing,[7] biological microtechnologies,[8] thin film formation, and coatings. Thus, efforts to understand the mechanisms of deposition during drying are both scientifically interesting and technologically useful. To date, the coffee-ring effect has been ameliorated in aqueous systems of large (>10 μm) suspended spheres,[9] in aqueous suspensions of ellipsoidal particles,[10] via electrowetting,[11] and in systems with strong attractive forces between particles and substrate.[12] The coffee-ring effect prevails, however, for most systems.

Marangoni flows from regions of low to high surface tension should, in principle, be present at the air−water interfaces of drying liquid drops. Temperature-driven Marangoni flows, for example, can result from evaporative-cooling-induced nonuniform interface temperatures that, in turn, produce gradients in surface tension.[13−16] Indeed, resultant radial flows toward the center of a drop have been found in small drops of octane.[17] In water, however, such temperature-dependent Marangoni flows are suppressed, in part because of tiny amounts of surface-active molecules usually present at the air−water interface (i.e., fewer than would be needed to cover the interface fully).[4,14,15,17]

Surfactants can affect deposition phenomena in a variety of ways. Early experiments found that when aqueous colloidal drops are mixed with the small ionic surfactant sodium dodecyl sulfate (SDS) the deposition patterns change.[4] More recently, in small confined droplets of organic solvent containing dissolved polymer, it was shown that surfactants can be employed to produce a relatively uniform deposition.[18] Surfactant-driven Marangoni flows were suggested to arise when the local concentration of surfactant molecules at the pinned contact line increased because of the coffee-ring effect, and as a result, the surface tension of the drop decreased locally; this gradient in surface tension was suggested to produce a continuous Marangoni flow toward the center of the drop. Such surfactant-driven Marangoni flows are phenomenologically different from the temperature-driven flows noted above, which are generally undone by the presence of surfactants.[17] In related interesting work, surfactant is sprayed onto the drop;[19,20] in this case, the surfactant exists in different phases interacting with air and liquid, and thermodynamic transitions between these different phases can then lead to complex patterns (e.g., patterns due to Marangoni−Bénard instabilities).

In this article, we quantitatively investigate the mechanism of a prototype small ionic surfactant, SDS, on the evaporation of aqueous colloidal systems and their resulting particle coatings. We employ video microscopy to study these evaporating droplets. The experiments demonstrate that small ionic

Received: December 14, 2011
Revised: February 6, 2012
Published: February 27, 2012

dx.doi.org/10.1021/la204928m | Langmuir 2012, 28, 4984−4988

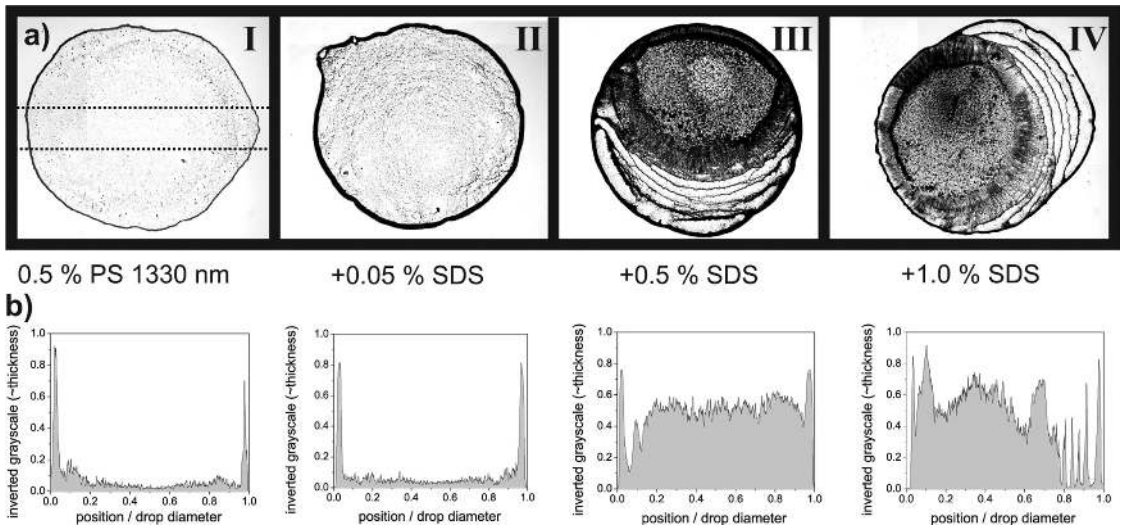

Figure 1. (a) Set of depositions from dried water drops containing 0.5 wt % PS particles (d = 1330 nm) and different concentrations of SDS (indicated under the pictures). The drops were evaporated on a hydrophilic microscope slide; the initial drop volume was about 0.05 L, and the resulting deposition area was between 1 and 2 mm in diameter. (b) Deposition profiles are shown under the corresponding pictures, averaged over 20% of the depositions diameter (i.e., within the dotted lines in aI). Note that the profile shows the inverted gray scale of the photographs, which is a useful relative measure of the deposition distribution in each picture but is not an absolute measure of the particle density.

surfactants such as SDS produce Marangoni flows in colloidal suspensions, thereby proving and visualizing the model suggested for polymer solutions.[18] Furthermore, these flows were discovered to produce a novel quasi-steady-state "eddy" that prevents most spheres from reaching the contact line and induces depinning of the contact line at later stages in the evaporation process. The experiments provide a first direct glimpse of surfactant-driven Marangoni effects in drying aqueous systems and illustrate how the Marangoni eddy can lead to significantly more uniform particle deposition. In addition, tree-ring deposition is observed and explained in this context.

EXPERIMENTAL METHODS

An evaporating liquid drop containing small solid particles and surfactant is a complex fluid system with many variables. Parameters that can be varied independently include the suspending liquid, the chemistry, size, polydispersity, shape, and concentration of the solid constituents, the type and concentration of surfactant, the properties of surfaces and interfaces, the drop size, and the temperature. Here we focus on a few representative systems of evaporating drops with the small ionic surfactant SDS, and we attempt to elucidate the rules governing their behavior.

The experiments employed aqueous suspensions of colloidal polystyrene (PS) particles with diameter d = 1330 nm. The particles were synthesized by surfactant-free radical emulsion polymerization and stabilized by sulfate groups.[21] Note that all reported findings were qualitatively verified using smaller PS particles (d = 415 nm) and silica particles ($d \approx$ 850 nm) synthesized by a modified Stoeber process.[22] Suspensions were prepared with deionized water and filtered with a Millipore column, and then the suspensions of PS spheres and sodium dodecyl sulfate (SDS, Sigma-Aldrich) (in different compositions) were thoroughly mixed by a vortex mixer and ultrasonicated for 5 min.

Evaporation experiments were performed using a brightfield microscope with air objectives (magnification 5× to 100×). Clean glass substrates (Fisher Scientific, hydrophilic) and polymer-coated microscope coverslips (Fisher Scientific, hydrophobic) were used as evaporation substrates. The drop volume was about 0.05 μL, leading to deposition coatings with diameters of 1 to 3 mm. The evaporation process was recorded with a video camera (658 pixels × 494 pixels) mounted on the microscope; the temporal resolution was 60 frames per second. Total evaporation times ranged between 2 and 4 min. At all concentrations, the experiment was repeated about 10 times, showing consistent concentration-dependent behavior. Photographs of the entire deposit, obtained after evaporation was complete, were taken by combining up to four photographs when the deposition area was larger than the microscope field of view.

RESULTS AND DISCUSSION

Results. Figure 1a shows top views of the deposition pattern of an aqueous suspension of PS spheres (0.5 wt %) (I) and with different concentrations of SDS ranging from 0.05 to 1.0 wt % (II–IV). Sample I exhibits classic coffee-ring deposition; most of the PS spheres are deposited at the edge of the drop. The corresponding graphs in Figure 1b show transmitted light intensity profiles of these samples; the intensity (vertical axis) is essentially proportional to the inverse of the gray scale in the pictures, which in turn corresponds to the concentration/layer thickness of the deposited particles. (As a first approximation, we assume a linear relationship between the gray scale and particle area concentration.) For the sample with no SDS, nearly all spheres are deposited in a thin ring located at the initial pinned contact line, and very few particles occupy the center of the drop. The addition of a small amount of SDS (0.05 wt %, picture II) slightly changes the resulting deposition. In sample II, the outer deposition ring is a little broader than in sample I and a slightly higher fraction of spheres is deposited in the center of the drop. A closer examination of the outer areas reveals several weak line patterns. Such patterns have been previously observed but are more delineated and more extensive than those of smaller particle suspensions used by Deegan.[4] Although a detailed explanation of these more subtle deposition pattern features is elusive, it is clear that they originate from a complex interplay of flow dynamics, capillary forces, and other instabilities.[19,20]

At much higher SDS concentrations (0.5 wt % (sample III) and 1.0 wt % (sample IV)), the deposition pattern changes dramatically. A ring at the initially pinned contact line persists at these high concentrations. Furthermore, both samples exhibit "tree-ring-like" structures with several distinct deposition lines

dx.doi.org/10.1021/la204928m | Langmuir 2012, 28, 4984–4988

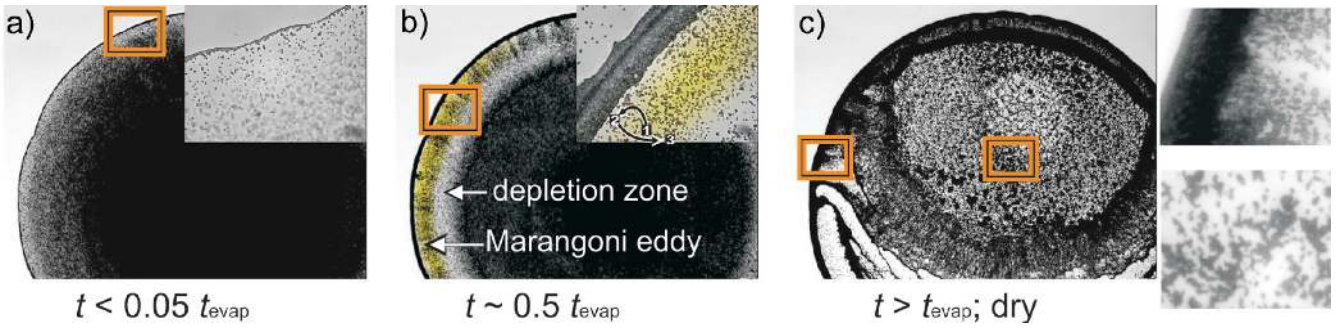

Figure 2. Snapshots during the evaporation of a water drop containing 0.5 wt % PS particles (d = 1330 nm) and 0.5 wt % SDS at magnifications of 5× (large) and 63× (insets) at different states in the drop evaporation (noted as a fraction of the total evaporation time t_{evap}): (a) $t \approx 0.05t_{evap}$. A line of spheres packs at the pinning line. In the 63× picture, it can be seen that the ring in this early state consist of only a few particles. (b) $t \approx 0.5t_{evap}$. The Marangoni eddy is highlighted yellow where particles from the bulk flow toward the edge but are repelled on the surface toward the center of the drop. In the 63× picture, the motion of an exemplary single sphere is highlighted by numbers 1−3, respectively, at the time of the picture, 0.25 s later (i.e., sphere next to the edge), and 0.5 s later (i.e., sphere repelled). Its trajectory is essentially given by two straight lines connecting the numbers (cf. Figure 3a). (c) $t > t_{evap}$ (i.e., completely dried). The 63× pictures show two different cutouts from the 5× picture (edge and center).

that cover about a third of the total area. Our evidence suggests that these tree-ring deposition structures result from depinning and repinning of the drop's contact line along a large part of the perimeter; after the drop shrinks, a new contact line stabilizes very quickly via self-pinning by other PS particles in suspension.[4] This effect occurs several times to produce the observed pattern. Far from the tree-ring-like structures, both systems exhibit relatively uniform depositions of spheres about their centers, surrounded by dark "flares".

We studied the temporal evolution of drops by video microscopy during evaporation in order to understand the deposition features of samples III and IV better. Figure 2 shows snapshots of the drying drop in Figure 1aIII (0.5 wt % SDS) at three different stages: (a) shortly after the drop is created, (b) at a time of about 50% of the total evaporation duration, t_{evap}, and (c) in the dry state. The regions highlighted by the rectangles are shown in insets at higher magnification. (Note that for stages a and b the higher-magnification pictures are taken from another similar drop because it was not possible to observe one individual drop with two different objectives simultaneously. For c, all three photographs are taken from the same deposition.)

When the evaporation starts, the drop behavior is identical to that of drops without SDS. Specifically, the contact line pins very quickly and spheres arrange in a densely packed structure at the edge. This behavior is clearly seen in the magnified picture, wherein deposition at the contact line consists of two to five rows of densely packed PS spheres. Particles in the bulk are uniformly distributed; therefore, the image gets increasingly dark toward the drop center where the drop is thickest.

However, a close examination of the pinned line reveals that even in the early stages of evaporation some spheres flow toward the edge but do not reach the edge. Rather, they appear to be repelled back toward the drop center as they approach the edge. In fact, with advancing evaporation time, the flow of particles toward the edge increases in magnitude over time,[4] and eventually all particles are repelled from the edge. Thus, the number of particles that approach the edge but do not reach it increases. The resultant behavior is the quasi-steady state and is shown in Figure 2b; a broad corona (i.e., an outer rim distinctly different and separated from the inner part of the drop) is observed between the relatively uniform dark center and the coffee-ring.

The dark part of the corona is perhaps best described as an eddy or circulating region of PS spheres transported toward and away from the drop edge throughout the drying process (marked as the Marangoni eddy in Figure 2b). PS spheres are pulled from the light zone (marked as the depletion zone in Figure 2b) into the eddy, leading to a locally reduced number of PS spheres in the depletion zone. The particle motions associated with the eddy are best visualized in our high-magnification video (Supporting Information), and the reader is strongly encouraged to view these supporting videos. Figure 2b shows the PS spheres participating in the eddy, but one cannot unambiguously ascertain their motions from a single still-life image. Nevertheless, we mark the motion of one sphere by numbers (1, 2, 3) in the magnified picture. The sphere is approximately in the center of the eddy at the time that Figure 2b is taken (1). After 0.25 s, the sphere is pushed radially outward toward the coffee ring but does not reach it (2). After an additional 0.25 s, the sphere is repelled toward the region between the eddy and the depletion zone (3). The corresponding video (Supporting Information) shows how more and more individual spheres join the eddy and how a few spheres are pushed radially inward so strongly that they move into or beyond the depletion zone, ultimately contributing to the uniform deposition.

Snapshots from the video at different stages within the lifetime of the eddy are shown in Figure 3. At $t \approx 0.28t_{evap}$ (Figure 3b), the eddy region (i.e., the region between two bars) is relatively thin and only a few spheres take part in the characteristic flow. As the local concentration of particles increases (Figure 3c−e), the number of small aggregates participating increases as well. A higher concentration of particles increases the probability of individual particles touching one another and building aggregates. The width of the eddy region and the number of particles involved in it are shown as functions of evaporation time in Figure 4. A clearly discernible eddy area is observed starting at about $t/t_{evap} = 0.2$; its width increases steadily, ranging from 35 to 70 μm at $t/t_{evap} \approx 0.5$, and then the width remains virtually constant (± 5 μm) until the contact line depins.

Because the absolute number of particles is hard to count in later stages, we estimate the particle density from the averaged gray scale of a standardized rectangle in the eddy area, normalized to its maximum value ρ_{max}. These particle number data, presented in Figure 4, reveal that the number of involved

dx.doi.org/10.1021/la204928m | Langmuir 2012, 28, 4984−4988

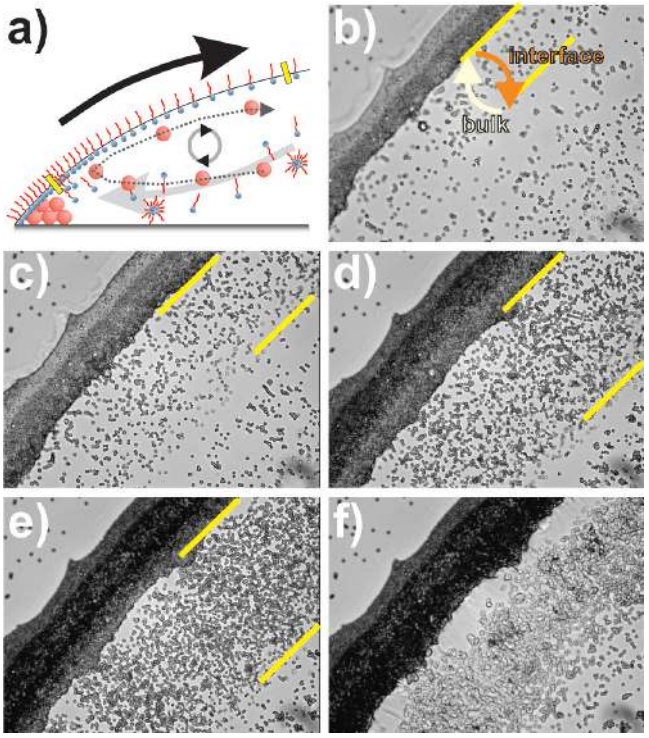

Figure 3. (a) Schematic description of the Marangoni eddy: SDS molecules from the bulk are pushed to the pinned contact line, where they try to reach the water/air interface. The locally increased surface concentration of SDS decreases the local surface tension and leads to a surface Marangoni flow toward the center of the drop. (b–f) The Marangoni eddy for a sample containing 0.5 wt % PS particles (1330 nm) and 0.5 wt % SDS at different stages in the evaporation. The edge of the drying drop is photographed at 63× magnification at (b) $t \approx 0.28t_{evap}$, (c) $t \approx 0.42t_{evap}$, (d) $t \approx 0.71t_{evap}$, (e) $t \approx 0.86t_{evap}$, and (f) $t > t_{evap}$ (dry).

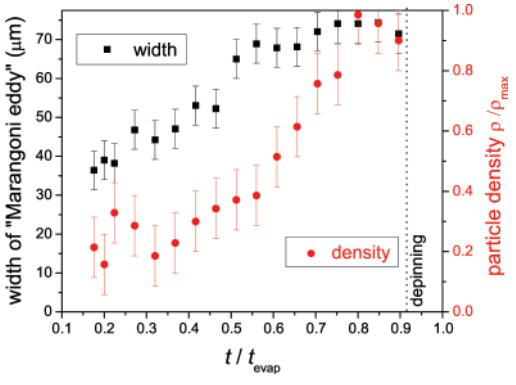

Figure 4. Width of the Marangoni eddy and the relative particle density inside the eddy area as a function of evaporation time for the experiment shown in Figure 3.

particles increases continuously until the contact line depins, leading to an increasing particle density in the eddy, especially at late times when the eddy stops broadening (thereby increasing the slope of $\rho(t)$ after $t > 0.5t_{evap}$). Note that the particles flowing toward the pinned contact line are mostly in the same plane as those already deposited at the edge (i.e., near the substrate) whereas the repelled particles are out of focus, implying that the repelled particles are closer to the air–water interface and are being swept back along the interface toward the drop center.

Eventually, when most of the water has evaporated, the contact line depins completely and particles are deposited relatively uniformly in the center of the drop. This uniform deposition is possible only because most of the particles could not reach the coffee ring in earlier stages of drying, as they would have done without the addition of SDS and the resulting Marangoni eddy.

Discussion. To the best of our knowledge, the present observations are the first real-time direct visualization of a surfactant-driven Marangoni effect. The phenomenon has recently been shown to alter the deposition of drying polymer solutions containing oligomeric fluorine-based surfactants.[18] It should be noted that the aqueous colloidal suspensions are quite different from previously studied polymer solutions; the former do not exhibit gelation[23] or a change in surface tension dependent on the local solute concentration, as described for the latter.[24,25]

Real-time visualization facilitates a comprehensive understanding of this mechanism, which is schematized in the side view in Figure 3a. An eddy region forms in between the yellow bars in Figure 3b–e in the top view. Just after a drop is created, some of the surfactant molecules (symbolized in the cartoon by a hydrophilic "head" with a hydrophobic "tail") populate the water/air interface. Note that although the interface is the preferred location for the amphiphilic SDS molecules their equilibrium packing is unlikely to be sterically dense because of the electrostatic repulsion of the anionic heads, and at a sufficiently high concentration, a significant number of SDS molecules can also be found to be dissolved in the bulk (i.e., freely or as micelles as depicted in Figure 3a).

When the contact line is initially pinned, the outward convective flow that is responsible for the coffee-ring effect transports spheres and SDS molecules to the drop edge. SDS molecules concentrate at the air–water interface near the contact line and locally decrease the interfacial surface tension γ. The surface tension gradient along the air–water interface, $\Delta\gamma$, thus created leads to a Marangoni flow along the drop air–water interface from low to high γ. The flow is strong enough to carry many colloidal spheres in the bulk, but near the interface, toward the drop center.

As these spheres move toward the center of the drop, where the local SDS concentration is lower (i.e., the local γ is higher), the Marangoni flow becomes weaker, and the outward convective flow that carries particles from the middle of the drop to the contact line dominates the Marangoni flow. Particles that travel to this point are pulled from the air–water interface to the drop center and carried toward the drop's edge once again; then the process repeats. Because these particles are trapped in the eddy and because new particles accrue from the central regions of the drop, the number of particles in the eddy increases with time as shown in Figure 4. SDS molecules are likely participating in the eddy as well; otherwise, the surface would become saturated, ending or weakening the Marangoni flow. The increasing width of the Marangoni eddy (Figure 4) presumably reflects the increasing total concentration of SDS due to the evaporation of water, consistent with our observation that higher initial SDS concentrations generally lead to broader eddies.

It is noteworthy that even at low concentrations (0.05 wt %) some particles are repelled from the contact line (as can be seen in high-magnification microscopy). However, the Marangoni flows become stronger at SDS concentrations above the critical micelle concentration (cmc) in water (8.3 mM ≈ 0.2 wt %[26]).

dx.doi.org/10.1021/la204928m | Langmuir 2012, 28, 4984–4988

We do not fully understand this effect. A possible explanation for this finding is that at the cmc the coverage of the air−water interface with SDS molecules is not sterically dense because of electronic repulsion and more SDS molecules can be pushed onto the interface. Note that if the surface packing of SDS becomes greater than it is in equilibrium at the cmc, then the resulting increased electronic repulsion between SDS molecules will favor the desorption of SDS.

Because the concentration of particles remains high in the eddy region (i.e., because they do not attach to the edge), repeated depinning and subsequent self-repinning leads to the tree-ring-like structures we found (Figure 1aIII,IV). When a new contact line is pinned, the Marangoni flow process restarts. When the final depinning occurs, many particles are left in the bulk because the eddy prevented them from attaching to the edge. Thus, when the line is finally depinned, the remaining spheres are deposited as the depinned contact line moves radially in, leading to a macroscopically uniform deposition in the center of the drop. Accordingly, the existence of the Marangoni eddy is a prerequisite of the "uniform" deposition in the central region because it prevents particles from depositing at the edge and thus delays the deposition of particles until the contact line is ultimately depinned.

Another interesting issue that we will not discuss quantitatively is the existence of particle-density inhomogeneities within the Marangoni eddy. Figure 2b reveals that the number of particles in the eddy is not uniform. In fact, alternating areas of higher and lower particle flux are found, which are surprisingly stable during the entirety of the eddy. This dynamic quasi-equilibrium in a highly nonequilibrium system is a challenge for future models.

CONCLUSIONS

We presented detailed observations and analyses of how small ionic surfactants, such as SDS, can lead to the more uniform deposition of spheres from drying aqueous colloidal drops. SDS on the air−water interface creates a strong Marangoni flow toward the center of a drop. Such a flow leads to a previously unreported Marangoni eddy of particles that prevents most of the spheres from reaching the contact line and finally supports the depinning of the contact line, ultimately leading to the uniform deposition of the remaining particles. Surfactants have been used for many years in industrial applications involving drying suspensions (e.g., ink jet printing[27,28]) and have often been applied in experience-based trial-and-error experiments. Herein, we have revealed one underlying mechanism by which surfactants can counteract the coffee-ring effect. This knowledge permits new insights into the complex system of drying suspensions and suggests pathways for a more purposeful and systematic utilization of surfactants in practical applications. Interestingly, preliminary experiments on large nonionic surfactants suggest a qualitatively different influence on drying suspensions, which will be discussed elsewhere.

ASSOCIATED CONTENT

Supporting Information

Video 1 shows the drying drop in Figure 2 (0.5% PS spheres, 0.5% SDS) at low magnification (5×) at 5 times the real velocity. Video 2 shows the initial phase of the Marangoni eddy in a drop of the same composition at high magnification (63×) in real time. This material is available free of charge via the Internet at http://pubs.acs.org.

AUTHOR INFORMATION

Corresponding Author

*E-mail: timstill@seas.upenn.edu.

Notes

The authors declare no competing financial interest.

ACKNOWLEDGMENTS

T.S. acknowledges the DAAD (German Academic Exchange Service) for a postdoctoral fellowship. We gratefully acknowledge financial support from the National Science Foundation through DMR-0804881, PENN MRSEC DMR11-20901, and NASA NNX08AO0G, and we thank Markus Retsch for the PS particles and M. Lohr, Ke Chen, A. Basu, M. Gratale, L. Hough, R. Murphy, and C. Cejas for helpful discussions.

REFERENCES

(1) Deegan, R. D.; Bakajin, O.; Dupont, T. F.; Huber, G.; Nagel, S. R.; Witten, T. A. *Nature* **1997**, *389*, 827.
(2) Denkov, N. D.; Velev, O. D.; Kralchevsky, P. A.; Ivanov, I. B.; Yoshimura, H.; Nagayama, K. *Nature* **1993**, *361*, 26.
(3) Hu, H.; Larson, R. G. *J. Phys. Chem. B* **2002**, *106*, 1334−1344.
(4) Deegan, R. D. *Phys. Rev. E* **2000**, *61*, 475−485.
(5) Bigioni, T. P.; Lin, X.-M.; Nguyen, T. T.; Corwin, E. I.; Witten, T. A.; Jaeger, H. M. *Nat. Mater.* **2006**, *5*, 265−270.
(6) Kaya, D.; Belyi, V. A.; Muthukumar, M. *J. Chem. Phys.* **2010**, *133*, 114905.
(7) Park, J.; Moon, J. *Langmuir* **2006**, *22*, 3506−3513.
(8) Yauk, C. L.; Berndt, M. L. *Environ. Mol. Mutagen.* **2007**, *48*, 380−394.
(9) Weon, B. M.; Je, J. H. *Phys. Rev. E* **2010**, *82*, 015305.
(10) Yunker, P. J.; Still, T.; Lohr, M. A.; Yodh, A. G. *Nature* **2011**, *476*, 308.
(11) Eral, H. B.; Augustine, D. M.; Duits, M. H. G.; Mugele, F. *Soft Matter* **2011**, *7*, 4954−4958.
(12) Sommer, A. P.; Rozlosnik, N. *Cryst. Growth Des.* **2005**, *5*, 551.
(13) Zhang, N.; Yang, W.-J. *J. Heat Transfer* **1982**, *104*, 656−662.
(14) Savino, R.; Paterna, D.; Favaloro, N. *J. Thermophys. Heat Transfer* **2002**, *16*, 562−574.
(15) Hu, H.; Larson, R. G. *Langmuir* **2005**, *21*, 3972−3980.
(16) Ristenpart, W. D.; Kim, P. G.; Domingues, C.; Wan, J.; Stone, H. A. *Phys. Rev. Lett.* **2007**, *99*, 234502.
(17) Hu, H.; Larson, R. G. *J. Phys. Chem. B* **2006**, *110*, 7090−7094.
(18) Kajiya, T.; Kobayashi, W.; Okuzono, T.; Doi, M. *J. Phys. Chem. B* **2009**, *113*, 15460−15466 .
(19) Nguyen, V. X.; Stebe, K. J. *Phys. Rev. Lett.* **2002**, *88*, 164501.
(20) Truskett, V. N.; Stebe, K. J. *Langmuir* **2003**, *19*, 8271−8279.
(21) Goodwin, J. W.; Hearn, J.; Ho, C. C.; Ottewill, R. H. *Colloid Polym. Sci.* **1974**, *252*, 464.
(22) Nozawa, K.; Gailhanou, H.; Raison, L.; Panizza, P.; Ushiki, H.; Sellier, E.; Delville, J. P.; Delville, M. H. *Langmuir* **2005**, *21*, 1516−1523 .
(23) Okuzono, T.; Kobayashi, M.; Doi, M. *Phys. Rev. E* **2009**, *80*, 021603.
(24) Poulard, C.; Damman, P. *Europhys. Lett.* **2007**, *80*, 64001.
(25) Kajiya, T.; Monteux, C.; Narita, T.; Lequeux, F.; Doi, M. *Langmuir* **2009**, *25*, 6934−6939 .
(26) Cifuentes, A.; Bernal, J. L.; Diez-Masa, J. C. *Anal. Chem.* **1997**, *69*, 4271−4274.
(27) Zhang, J.; Li, Z.; Dong, C. *China Surfactant Deterg. Cosmet.* **2004**, *2004*, 381.
(28) Socol, Y.; Guzman, I. S. *J. Phys. Chem. B* **2006**, *110*, 18347−18350.